# Phase separation to antiferromagnetic and superconducting domains in oxygen-rich single-crystal $La_2CuO_{4+x}$: Magnetic and structural neutron-diffraction studies

D. Vaknin, J. L. Zarestky, and D. C. Johnston
*Ames Laboratory and Department of Physics and Astronomy, Iowa State University, Ames, Iowa 50011*

J. E. Schirber
*Sandia National Laboratories, Albuquerque, New Mexico 87185*

Z. Fisk
*Los Alamos National Laboratory, Los Alamos, New Mexico, 87545*
(Received 28 July 1993; revised manuscript received 16 November 1993)

We report on magnetic and structural neutron-diffraction studies of single-crystal $La_2CuO_{4+x}$ versus temperature. The low-temperature diffraction data are consistent with the coexistence of two structurally related phases: nearly stoichiometric, antiferromagnetic (AF) domains, with average domain diameter $\sim$ 500 Å in the $CuO_2$ plane, and oxygen-rich, metallic, and superconducting domains. The ordered magnetic moment in the AF domains does not saturate at 10 K, and is on average, $\mu = (0.3 \pm 0.05)\mu_B$/Cu atom. The phase-separation transition to these two phases occurs at $T_{PS} = 260 \pm 5$ K, which is about 15 K higher than the Nèel temperature, $T_N = 245 \pm 3$ K. The value of $T_{PS}$ is identical within the errors with that ($259 \pm 2$ K) found previously from specific-heat measurements on the same crystal. The structural properties of the single crystal are discussed and compared to those of polycrystalline oxygen-rich $La_2CuO_{4+x}$.

## I. INTRODUCTION

$La_2CuO_4$, the parent material of the cuprate superconductors $La_{2-y}Ba_yCuO_4$ (Ref. 1) and $La_{2-y}Sr_yCuO_4$ (Ref. 2), is an insulating antiferromagnet[3,4] with an electronic configuration that is very unstable to a variety of dopants.[5] The superconducting state arises by a modest ($y \geq 0.1$) substitution of the trivalent atom, La, by the divalent atoms Ba or Sr. A smaller level of substitution ($y \geq 0.02$) with Sr or Ba, although not yielding a superconducting state, completely destroys the long range antiferromagnetic (AF) order, driving the system into a spin-glass-like state.[6–8] Doping of this system can also be obtained by introducing excess oxygen in interstitial sites[5] to produce $La_2CuO_{4+x}$, or by photodoping processes.[9] The bulk oxygen doping can attain $x \approx 0.12$.[10] However, even for levels of doping $x < 0.06$, superconductivity is observed and the spin-glass-like behavior is missing, in contrast to the substitutional doping.

Numerous structural and electronic studies of oxygen-rich $La_2CuO_{4+x}$ all indicate that a structural phase separation to stoichiometric and to oxygen-rich domains occurs at a temperature $T_{PS}$ around room temperature.[5,10–17] Neutron- and x-ray-diffraction measurements of polycrystalline oxygen-rich $La_2CuO_{4+x}$ (Refs. 11 and 12) show that at low temperatures, the symmetries of the two phases are consistent with space groups *Bmab*, stoichiometric, and *Fmmm*, oxygen rich and superconducting. By contrast, a single-crystal neutron-diffraction study[13] suggests that the oxygen-rich rich phase is of *Bmab* symmetry, and that the excess oxygen atoms reside between successive LaO layers. Recent studies of the pure superconducting $La_2CuO_{4+x}$ phases, prepared by electrochemical oxidation ($x$=0.08, 0.1, and 0.12), indicate that the crystallographic structure of all samples has *Fmmm* symmetry with extra reflections suggestive of a very large superlattice structure, and no phase separation was observed down to 10–18 K.[10] Muon spin rotation experiments[14] on polycrystalline samples ($x \approx 0.03$) reported that more than half of the sample undergoes superconductivity with $T_c$=35 K and the other part displays static AF ordering, similar to that of stoichiometric $La_2CuO_4$. Subsequently, $^{139}$La NMR studies[15] on a single crystal of $La_2CuO_{4+x}$ showed two signals, one attributed to stoichiometric domains ($x$=0) and the other to oxygen-rich domains ($x > 0$). The disappearance of the signal associated with the oxygen-rich domains above 265 K, and the anomalies near $T_{PS}$ in the anisotropic electronic transport and magnetic susceptibility measurements,[16] suggested that the transition may be driven, at least in part, by copper spin magnetism. These studies[16] also showed a hysteresis in the temperature dependence of the electronic transport and the magnetic susceptibility $\chi(T)$ near $T_{PS}$, classifying the transition as a weakly first order process. Based on theory, it has been concluded that this segregation of the excess oxygen atoms is mediated by a strong electronic instability in the $CuO_2$ planes arising from the doping of holes[18,19] and not by an elastic mechanism. Emery and Kivelson have recently argued that in the case of oxygen doping, the doped holes together with the oxygen dopants behave more like uncharged immiscible entities in the AF host, while the divalent dopants (Sr, Ba, etc.) are fixed and create charged holes that participate

 

in a *frustrated phase separation.*[19] Thus, it is by virtue of their high mobility that the excess interstitial oxygen atoms in the $La_2CuO_{4+x}$ phase separate together with doped holes.

The understanding of this transition has received considerable attention recently, as it becomes evident that the mechanism involved in the formation of phase-separated domains may shed light on missing ingredients for the formulation of a model that appropriately describes the delicate and rich electronic properties of the cuprate superconductors.[19] The introduction of excess oxygen into $La_2CuO_4$ is a very subtle perturbation of the stoichiometric state that may help probe the mechanism that drives the doped system into the superconducting state. It is widely believed that any model for the superconducting state of the cuprates must be sufficiently universal to adequately describe both the undoped and the lightly doped materials.

The objective of the present study has been to test these ideas, by correlating structural and magnetic neutron-diffraction measurements on a superoxygenated $La_2CuO_{4+x}$ single crystal. To our knowledge such combined measurements have not been performed before on the same polycrystalline or single-crystal sample. Further, magnetic neutron-diffraction measurements have not been reported in phase-separated $La_2CuO_4$. Our primary objectives were to determine whether or not $T_{PS}$ and $T_N$ were the same and, if so, whether there is a discontinuous change in the ordered moment at $T_N$. Magnetic-susceptibility and specific-heat measurements on the same crystal as used here indicated that $T_{PS} = 259 \pm 2$ K for this crystal.[17] The weak ferromagnetic peak in $\chi(T)$ of pure $La_2CuO_4$ due to Dzyaloshinsky-Moriya type of interactions[20] is greatly suppressed in magnitude in this sample.[17] The zero-field-cooled $\chi(T)$ data indicate that superconductivity occurs below $T_c = 35$ K, and that at least half of the crystal is superconducting at 5 K. High resolution synchrotron x-ray-diffraction studies of powdered samples[12] indicate that the phase separation manifests itself by the splitting of the (006) Bragg reflection. Examining the results of Ref. 12, under the conditions of our poorer resolution, we noticed that in addition to the expected broadening of the combined (006) reflections, the total integrated intensity also increases significantly below $T_{PS}$. In this study we adopted the approach of monitoring the temperature dependence of the intensities and linewidths of several Bragg reflections to determine $T_{PS}$.

Our paper is organized as follows: In Sec. II we describe the experimental procedures and the setup used during the scattering experiments. In Sec. III we give the results and analysis of the structural and magnetic neutron-diffraction experiments, and in Sec. IV we discuss our results and compare them to theories and other experiments and conclude by giving the implications of our results in regard to the current state of understanding of the phase-separation transition.

## II. EXPERIMENTAL DETAILS

A single crystal of $La_2CuO_4$ of mass 72.8 mg was grown in a CuO flux as described previously.[16] The irregularly shaped crystal was annealed at 3 kbar $O_2$ pressure and 575 °C for 12 h, followed by cooling to room temperature at a rate of about 100 °C per hour. From previous work on similarly prepared crystals,[16] the oxygen excess in the resulting $La_2CuO_{4+x}$ crystal is estimated to be $x \cong 0.03$. The $La_2CuO_{4+x}$ crystal is the same one used for heat-capacity (150–300 K) and anisotropic magnetic-susceptibility (5–300 K) measurements in Ref. 17 as noted above.

Neutron-diffraction measurements were carried out on the triple axis spectrometer HB1A at the High Flux Isotope Reactor (HFIR) at Oak Ridge National Laboratory. A monochromatic neutron beam of wavelength $\lambda = 2.352$ Å was selected from the white beam by a double monochromator system using the (200) planes of a highly oriented pyrolytic graphite (HOPG) crystal, and analyzed by a second HOPG crystal after scattering from the sample. The $\lambda/2$ component in the beam was discriminated against to better than 3 parts in $10^4$ by a set of HOPG crystals as a filter between the two monochromators. The sample was wrapped in Al foil, sealed in a He environment, and mounted in a Displex closed cycle refrigerator. Two collimating configurations were used, 60′-20′-34′-136′ and 60′-80′-68′-136′, the first for the determination of the magnetic moment form factor at $T=$ 9.2 K, and the second for the temperature dependence studies. The sample was placed with its $a$ and $c$ axes in the scattering plane (for the sake of consistency we use the *Bmab* notation used in Refs. 11 and 12 in which $b \geq a$ and $c \gg a, b$). Due to twinning below the tetragonal to orthorhombic transition at $T_0 \simeq 350$ K, a $(hkl)$ reflection is almost superimposed with a $(khl)$ reflection.

## III. RESULTS AND ANALYSIS

### A. Nuclear scattering

To obtain structural information as a function of temperature, the (200), (020), (006), and (014) nuclear Bragg reflections were monitored in the temperature range 9.2–400 K. At 9.2 K, a set of reflections of the type $(0kl)$, $k$=1,3,5 and $l$=2,4 is observed implying the unequivocal presence of the *Bmab* phase. All these reflections have a linewidth broader than the resolution of the spectrometer. Whereas the detection of the low symmetry phase, *Bmab*, is straight forward, the detection of the oxygen-rich *Fmmm* phase is indirect. This is primarily due to extensive overlap of all Bragg reflections of the *Fmmm* phase with some of those of the *Bmab* phase. According to Refs. 11 and 12, at $T=$ 10 K, both phases maintain the same value for the lattice parameter $a$, whereas the $b$ and $c$ values of both phases differ, $(1-b_{Fmmm}/b_{Bmab} \simeq 0.004, 1-c_{Bmab}/c_{Fmmm} \simeq 0.0033)$. An additional obstacle in resolving the symmetry of the oxygen-rich phase is the intrinsic broadening of Bragg reflections beyond the resolution of the spectrometer due to possible domain size broadening effects, strain, and disorder in the distribution of excess oxygen atoms in the metallic phase.

Figure 1(a) shows the temperature dependence of the $a$ and $b$ in-plane lattice parameters extracted from the (200), (020), and (014) reflections. The value of the lattice parameter $b$, at 9.2 K, falls between those of the $b_B$ and $b_F$ values determined in the higher resolution studies of Refs. 11 and 12, where $b_B$ and $b_F$ are the lattice constants in the *Bmab* and *Fmmm* phases, respectively. The $b$ values (based on those found in Refs. 11 and 12) for the *Bmab* and *Fmmm* phases in the temperature range of 10–250 K are shown with a dashed line in Fig. 1(a). Similarly, Fig. 1(b) shows the temperature dependence of the $c$-axis lattice parameter extracted from the (006) Bragg reflection. Figures 2(a) and 2(b), respectively, show the temperature dependence of the intensity and the linewidth of the same (006) reflection, analyzed with a single Gaussian. The dashed line in Fig. 2(a) is the calculated temperature dependence of the (006) reflection intensity due to the Debye-Waller factor,[21] using the Debye temperature $\Theta_D = 385$ K for $La_2CuO_4$ obtained from low-temperature specific-heat measurements.[22] Both the integrated intensity and the linewidth as a function of temperature indicate a prominent change below $\approx$ 260 K. From previous work,[11,12] we attribute the increased broadening below $\approx$ 260 K to the presence of overlapping reflections arising from the coexistence of two phases with slightly different $c$ parameters. We have also observed some broadening of the mosaic spread of the (006) reflection upon cooling from room temperature to 10 K. The solid circles ($T$=9.2 K) in Fig. 1(b) are obtained from a fit to the (006) reflection assuming that the peak consists of two Gaussians (both with fixed linewidths, 0.035 $Å^{-1}$), consistent with the $c$ lattice parameters obtained in Refs. 11 and 12 at similar temperatures. From this analysis of the (006) reflection we estimate that at 10 K our crystal consists of about 35–45 % of the oxygen-rich metallic phase.

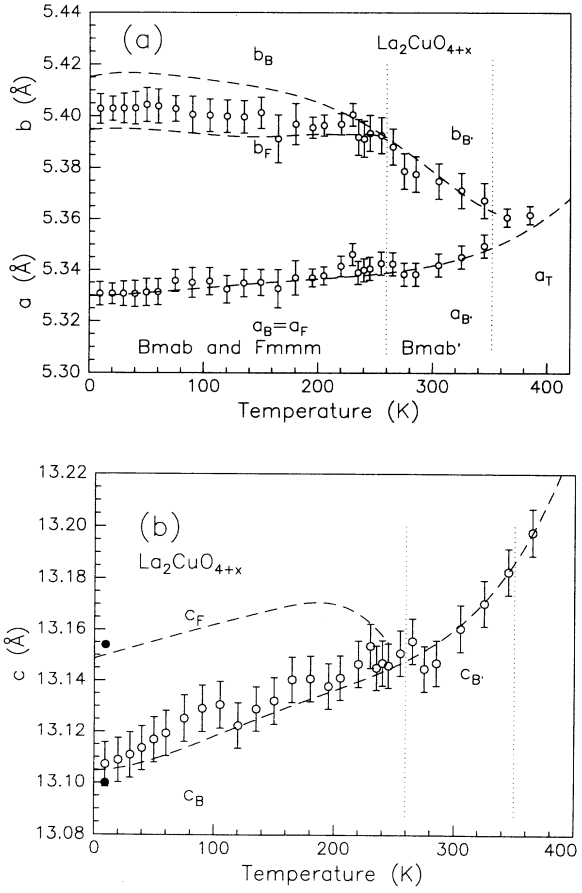


FIG. 1. Lattice constants vs temperature in $La_2CuO_{4+x}$ deduced from the neutron-diffraction data. The dashed lines representing the $b$ and $c$ lattice parameters for the two phases at temperatures below 260 K are reconstructed from Refs. 11 and 12. The solid circles in (b) are deduced from the (006) reflection assuming the superposition of two Gaussians (see text). Abbreviations: $T$ (tetragonal phase), $F$ (*Fmmm* phase), $B$ and $B'$ (*Bmab* phase).

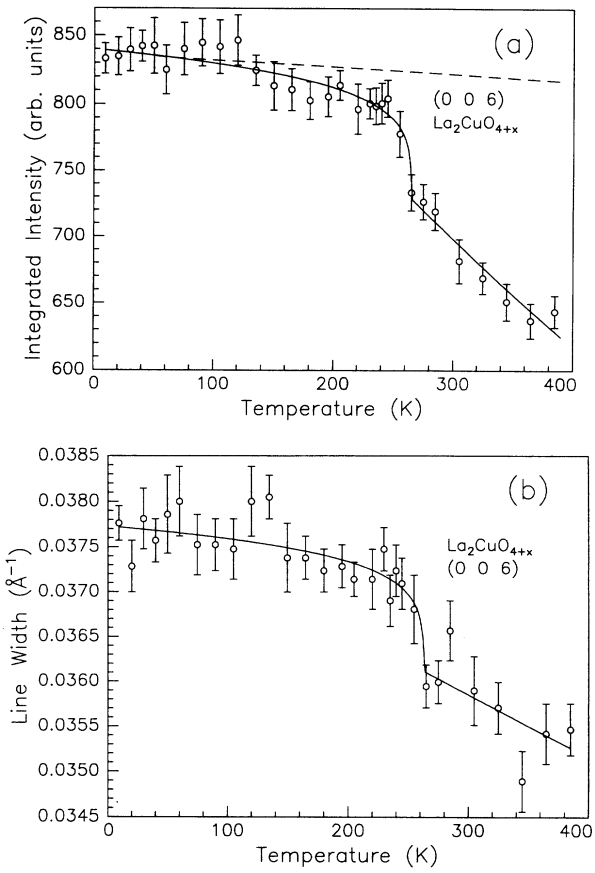


FIG. 2. Integrated intensity (a) and linewidth (b) vs temperature of the (006) reflection in $La_2CuO_{4+x}$. The dashed line in (a) is the expected temperature dependence due to the Debye-Waller factor (see text). The solid lines are guides to the eye.

The temperature dependences of the integrated intensity and the linewidth of the (014) reflection are shown in Figs. 3(a) and 3(b), respectively. The anomaly in the temperature dependence near 260 K in Fig. 3(a) is reproducible upon reheating the sample from 10 K. The (014) reflection arises as a result of a rigid rotation of the $CuO_6$ octahedra, and provides unequivocal evidence for the orthorhombic distortion and the presence of a phase with the *Bmab* space group. This rigid rotation of the $CuO_6$ octahedra occurs around the $(1,\bar{1},0)$ tetragonal

($I4mmm$) axis, with neighboring octahedra alternating in the direction of the tilt. The tilt angle, to a first order approximation, is proportional to the absolute value of the structure factor of the (014) reflection. Thus, the tilt angle can be regarded as an order parameter for the tetragonal-orthorhombic phase transition for the near-stoichiometric phase with $x \approx 0$. Below $T_{PS}$ and in the oxygen-rich phase with $x > 0$, assuming a $Bmab$ symmetry for this phase, this order parameter would be affected by the interstitial oxygen atoms which disrupt locally the tilt angle of the octahedra, consequently destroying the coherence length of the order parameter.

The broadening of the (014) reflection at low temperatures [cf. Fig. 3(b)] is either due to small-domain broadening effects of the $Bmab$ stoichiometric phase, and/or due to the possibility that the second phase is actually of the same $Bmab$ symmetry with slightly different lattice parameters,[13] rather than of $Fmmm$ symmetry.[11,12] Our measurements do not have the resolution necessary to distinguish between the two possibilities. Assuming that the broadening of the (014) reflection, over the resolution of the spectrometer, is predominantly due to small domain broadening effects in the AF $Bmab$ phase, we deduce an average diameter of 450 Å per domain. On the other hand, rationalization of the broadening of the (014) peak in terms of two adjacent reflections would require that the oxygen-rich phase have a symmetry lower than $Fmmm$. This possibility is consistent with the temperature dependence of Fig. 3(b) which is qualitatively similar to that of the (006) reflection [Fig. 2(a)] that has been explained in terms of two overlapping reflections. We have eliminated the possibility that the antiferromagnetic (see below) (104) reflection intensity, which is superimposed with the (014) reflection due to the twinning dis-

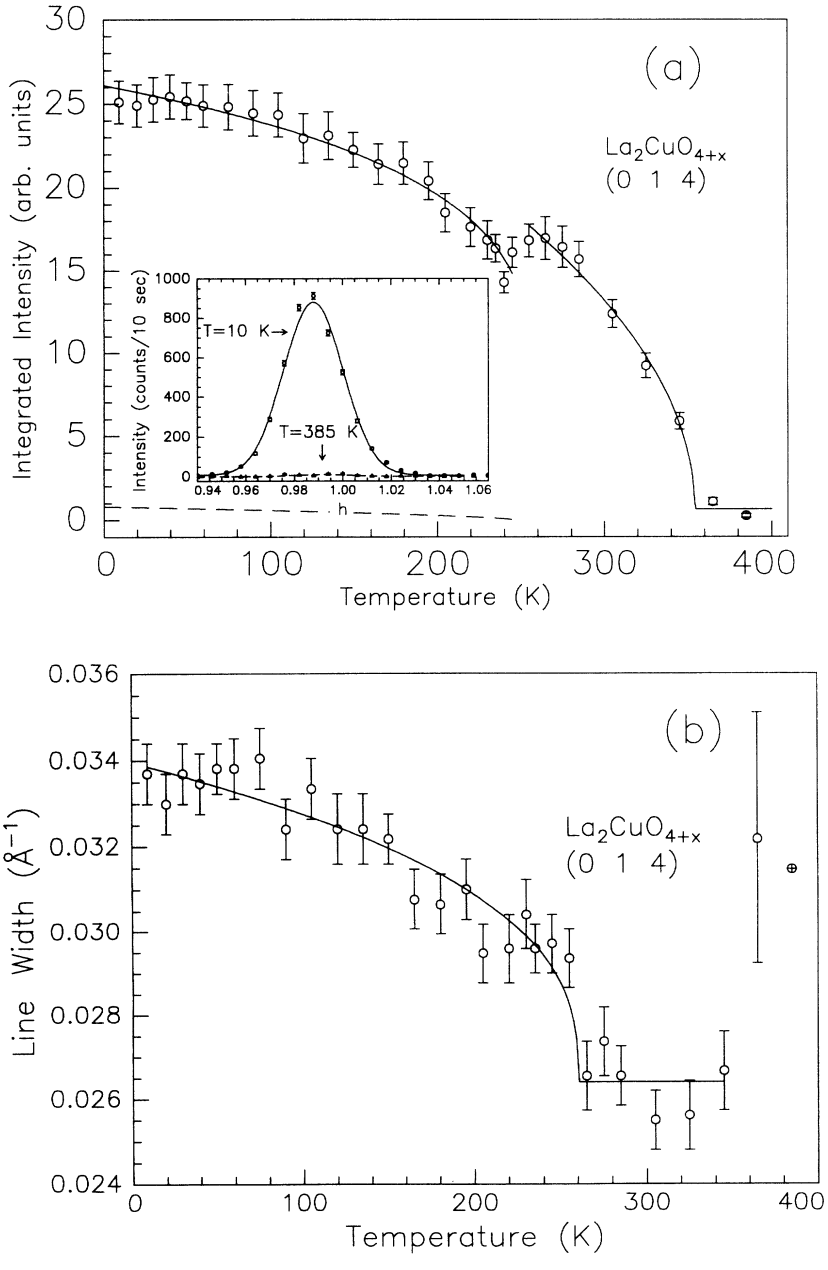


FIG. 3. (a) Integrated intensity and (b) linewidth vs temperature of the (014) nuclear peak. The solid lines are guides to the eye. The dashed line in the lower part of (a) is the calculated contribution of the antiferromagnetic (104) reflection. The inset in (a) shows the (014) reflection at two temperatures.

cussed above, contributes to the dramatic changes shown in Figs. 3(a) and 3(b). The dashed line in Fig. 3(a) represents the calculated contribution of the magnetic (104) reflection [based on the antiferromagnetic (100) reflection intensity discussed below] and is negligible.

The intensities and the linewidths of both the (006) and the (014) reflections, shown in Figs. 2 and 3 above, all show anomalous changes below $\approx 260$ K. As discussed above, these observations can be rationalized as due to phase separation into the near-stoichiometric AF phase and the oxygen-rich metallic and superconducting phase. From Figs. 2 and 3, we conclude that the phase separation temperature is $T_{PS} = 260 \pm 5$ K for our crystal. This value confirms the previous assignment of a specific-heat anomaly in this crystal at $259 \pm 2$ K to the phase separation transition.[17] Our $T_{PS}$ value is close to that ($265 \pm 5$ K) determined using $^{139}$La nuclear quadrupole resonance (NQR) for a similarly prepared crystal.[15]

The orthorhombic to tetragonal ($I4mmm$) transition occurs at $T_0 = 360 \pm 10$ K as is apparent from Fig. 3(a). The increase in the linewidth of the (014) reflection above 330 K implies a decreasing coherence length close to the transition, indicative of a second order tetragonal to orthorhombic phase transition. This $T_0$ is much lower than that of the stoichiometric material [$T_0 = 530$ K (Refs. 4 and 5)], and it is even lower compared to that ($T_0 \sim 420$ K) of the polycrystalline oxygen-rich samples studied in Refs. 11 and 12. On the other hand, our $T_0$

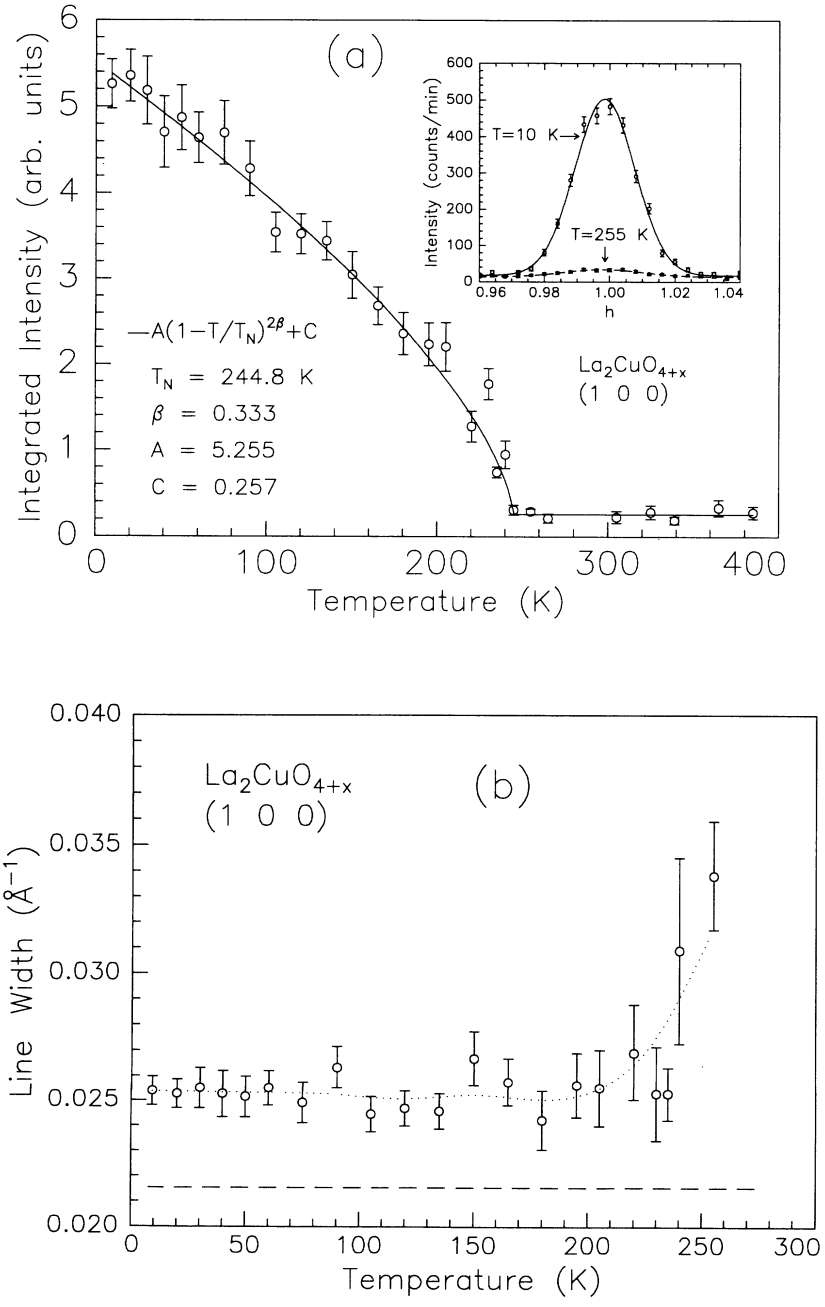


FIG. 4. Integrated intensity (a) and linewidth (b) vs temperature of the magnetic (100) reflection. The inset in (a) shows the reflection at 10 K and at 255 K. The solid curve below $T_N$ in (a) is a nonlinear least-squares fit to the data with the power law function shown. A remanant intensity at 255 K is due to the $\lambda/2$ contamination, in the neutron beam, from the nuclear (200) and (020) reflections. The dotted line in (b) is a guide to the eye, and the dashed lined represents the resolution of the spectrometer.

value is essentially identical to that found for a powder sample with $x \simeq 0.043 \pm 0.01$ in the structural phase diagram study of Ref. 23.

### B. Magnetic scattering

The magnetic properties of nearly stoichiometric $La_2CuO_{4+x}$ have been extensively investigated with the neutron-scattering technique.[4,5] They all indicate that an antiferromagnetic phase occurs below a Néel temperature $T_N \sim 50$–$300$ K, with an ordered magnetic moment $\mu \sim (0.2$–$0.6)\mu_B$/Cu atom, varying with oxygen content. Figure 4(a) shows the temperature dependence of the integrated intensity of the (100) reflection originating from the AF phase in our $La_2CuO_{4+x}$ crystal. We find further support for the magnetic origin of the (100) reflection in the observation of a variety of extra reflections that emerge at the same temperature. The relative intensities of these reflections are consistent with the antiferromagnetic spin structure suggested in Ref. 4. The temperature dependence of the integrated intensity of the (100) reflection is qualitatively similar to the ones reported for the similar systems $Ca_{0.85}Sr_{0.15}CuO_2$ (Ref. 24) and $Sr_2CuO_2Cl_2$.[25] The solid line in Fig. 4(a) is a fit to the experimental data with the power law function, $I = A(1 - T/T_N)^{2\beta} + C$. The parameters obtained from a nonlinear least-squares fit are listed in Fig. 4(a). We find $T_N = 245 \pm 3$ K for the AF phase in our crystal, which is about 15 K lower than $T_{PS}$ determined above. Minute remnant intensity at the nominal position of the (100) reflection, about 1 part in $10^4$ of the (200) intensity, observed above $T_N$, is attributed to the (020) and (200) reflections, due to the $\lambda/2$ component present in the beam. The calculated ordered magnetic moment, is $(0.30 \pm 0.05)\mu_B$/Cu atom assuming a value of 0.9 for the $Cu^{2+}$ magnetic form factor for the (100) magnetic reflection, and assuming that the antiferromagnetic phase constitutes 60% of the sample volume as estimated above.

Figure 5 shows the scattering wave-vector dependence of the magnetic form factor of $Cu^{2+}$ as deduced from the magnetic reflections [(1 0 0), (0 1 1), (1 0 2), (0 1 5), (3 0 0), and (3 0 1)] using the model proposed in Ref. 4. The solid line is a nonlinear least-squares fit to the zero order Bessel function, $j_0(qR_0)$, where $q$ is the modulus of the scattering vector and $R_0$ is an average radius within which the moment is localized. The value $R_0 \approx 0.55$ Å implies a moment that is localized within the ionic radius of $Cu^{2+}$, 0.69 Å.

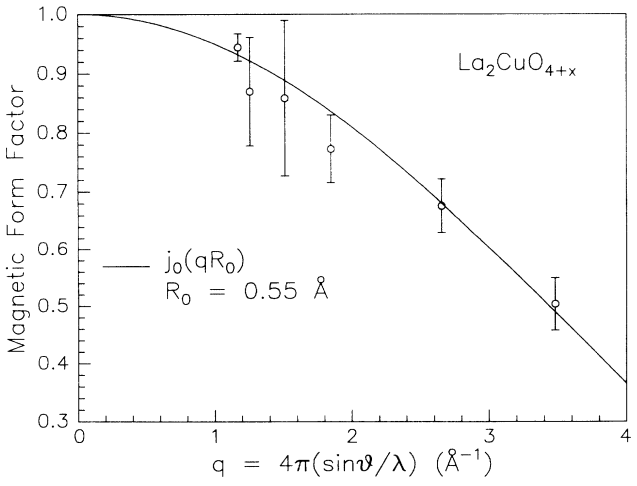


FIG. 5. The antiferromagnetic form factor of $Cu^{2+}$ in $La_2CuO_{4+x}$. The solid curve is a fit to the zero order Bessel function as indicated in the figure.

Figure 4(b) shows the temperature dependence of the linewidth of the (100) magnetic reflection. The dashed line below the experimental points indicates an upper limit to the value of the instrumental resolution for that scattering vector.[26] From the broadening of the linewidth, we estimate the magnetic domains to be $\approx 350$–$500$ Å in diameter within the $CuO_2$ plane at low temperatures, consistent with the value $\sim 450$ Å deduced above from the (014) nuclear reflection. In contrast to the temperature dependence of the integrated intensity of the (100) reflection, the linewidth in Fig. 4(b) is practically independent of temperature, except close to $T_N$, implying a second order phase transition.

## IV. DISCUSSION AND CONCLUSIONS

In our neutron-diffraction investigations of an oxygen-rich $La_2CuO_{4+x}$ single crystal, we have conclusively confirmed the microscopic nature of the phase-separation transition. We show that the near-stoichiometric domains (of the *Bmab* phase) are antiferromagnetically ordered and that the phase-separation transition temperature $T_{PS} \approx 260 \pm 5$ K is about 15 K higher than $T_N = 245 \pm 3$ K. This is consistent with a picture in which the holes in oxygen-rich $La_2CuO_{4+x}$ are expelled from the dynamically ordered antiferromagnetic regions, dragging with them the interstitial oxygen atoms which aggregate, in accordance with the general ideas developed by Emery, Kivelson, and Lin.[18,19] According to the theory, short-range order in the magnetic fluctuation regime above $T_N$ is sufficient to induce the phase separation. A hole together with its oxygen dopant in oxygen-rich $La_2CuO_{4+x}$ are practically chargeless, and tend to phase separate from the remaining undoped Cu spin system. By aggregating, the holes break fewer antiferromagnetic bonds between spins than if they are distributed statistically. This picture is consistent with the inference that phase separation is frustrated in the $La_{2-x}Sr_xCuO_4$ system, where instead the doped holes become inhomogeneously distributed on a nanoscopic length scale.[7,8]

An alternative explanation is that the phase separation may be elastically driven. One may argue that defects in the staggered tilt angle of the Cu-O octahedra, introduced by the presence of interstitial oxygen, may play the role that the holes play in the AF background, as discussed above. That is, the system minimizes its elastic energy by accumulating the defects, i.e., expelling the oxygen atoms from the coherent regions of tilted octahedra. The large dip in the integrated intensity of the (014) reflection supports the idea that the phase separation is intimately related to the tilt angle of the octahedra. Consequently, the holes will be dragged with the oxygen

atoms and allow for the AF order to develop in hole-free regions. However, the preponderance of evidence to date indicates that the phase separation is electronically driven.[19] Both pictures for the mechanism to drive the phase separation can be regarded as a general tendency of two different entities to minimize their surface of interaction, by segregating into domains. Thus, $N$ holes and/or defects break $N$ AF and/or staggered-tilt bonds, whereas the same $N$ holes and/or defects, aggregated in domains, break roughly $\sqrt{N}$ bonds, since essentially only those on the periphery of the domain break bonds (assuming the AF and/or staggered-tilt system is two dimensional). Either type of reorganization would give rise to the observed first order phase-separation transition.

From the linewidth of the magnetic (100) reflection at low temperature, we infer that the average diameter of the AF regions is about 500 Å parallel to the $CuO_2$ planes. This size is on the same order as that observed in dark-field electron microscope images,[27] where, however, the domains were found to have a high aspect ratio parallel to the $CuO_2$ planes. Our measurements provide no direct information about the size of the metallic phase domains at low temperatures. In contrast to our single-crystal data, neutron-diffraction studies of powders indicated that the average diameter of the AF regions was $>$ 5000 Å, whereas that of the metallic phase was either in this limit or, for one sample, was $\approx$ 3000 Å.[11] It is likely that the domain sizes and shapes depend on the excess oxygen content $x$ as well as on the thermal history of the samples, and possibly on the crystallite size.

## ACKNOWLEDGMENTS

We are grateful to F. C. Chou, V. J. Emery, J. D. Jorgensen, and P. G. Radaelli for helpful discussions. D.V. and J.L.Z. thank the ORNL neutron-scattering group for the hospitality extended during the performance of the neutron-scattering experiments. Ames Laboratory is operated by Iowa State University for the U.S. Department of Energy under Contract No. W-7405-Eng-82. This work was supported by the Director for Energy Research, Office of Basic Energy Sciences. The work performed at Sandia National Laboratories was supported by the U.S. Department of Energy under Contract No. DE-AC04-76DP00789 and at Los Alamos under the auspices of the U.S. Department of Energy Office of Basic Sciences.

[1] J. G. Bednorz and K. A. Müller, Z. Phys. B **64**, 89 (1986).
[2] R. J. Cava, R. B. van Dover, B. Batlogg, and E. A. Rietman, Phys. Rev. Lett. **58**, 408 (1987).
[3] D. C. Johnston, J. P. Stokes, D. P. Goshorn, and J. T. Lewandowski, Phys Rev. B **36**, 4007 (1987).
[4] D. Vaknin, S. K. Sinha, D. E. Moncton, D. C. Johnston, J. M. Newsam, C. R. Safinya, and H. E. King, Jr., Phys. Rev. Lett. **58**, 2802 (1987).
[5] For a review, see D. C. Johnston, J. Magn. Magn. Mater. **100**, 218 (1991).
[6] A. Aharony, R. J. Birgeneau, A. Coniglio, M. A. Kastner, and H. E. Stanley, Phys. Rev. Lett. **60**, 1330 (1988).
[7] J. H. Cho, F. Borsa, D. C. Johnston, and D. R. Torgensen, Phys. Rev. B **46**, 3179 (1992).
[8] J. H. Cho, F. C. Chou, and D. C. Johnston, Phys. Rev. Lett. **70**, 222 (1993); F. C. Chou, F. Borsa, J. H. Cho, D. C. Johnston, A. Lascialfari, D. R. Torgensen, and J. Ziolo, *ibid.* **71**, 2323 (1993).
[9] Y. H. Kim, C. M. Foster, A. J. Heeger, S. Cox, and G. Stucky, Phys. Rev. B **38**, 6478 (1988).
[10] P. G. Radaelli, J. D. Jorgensen, A. J. Schultz, B. A. Hunter, J. L. Wagner, F. C. Chou, and D. C. Johnston, Phys. Rev. B **48**, 499 (1993).
[11] J. D. Jorgensen, B. Dabrowski, S. Pei, D. G. Hinks, L. Soderholm, B. Morosin, J. E. Schirber, E. L. Venturini, and D. S. Ginley, Phys. Rev. B **38**, 11 337 (1988).
[12] P. Zolliker, D. E. Cox, J. B. Parise, E. M. McCarron III, and W. E. Farneth, Phys. Rev. B **42**, 6332 (1990).
[13] C. Chaillout, S-W. Cheong, Z. Fisk, M. S. Lehmann, M. Marezio, B. Morosin, and J. E. Schirber, Physica C **158**, 183 (1989); C. Chaillout, J. Chenavas, S-W. Cheong, Z. Fisk, M. Marezio, B. Morosin, and J. E. Schirber, *ibid.* **170**, 87 (1990).
[14] E. J. Ansaldo, J. H. Brewer, T. M. Riseman, J. E. Schirber, E. L. Venturini, B. Morosin, D. S. Ginley, and B. Sternlieb, Phys. Rev. B **40**, 2555 (1989).
[15] P. C. Hammel, A. P. Reyes, Z. Fisk, M. Takigawa, J. D. Thompson, R. H. Heffner, S-W. Cheong, and J. E. Schirber, Phys. Rev. B **42**, 6781 (1990); P. C. Hammel, E. T. Ahrens, A. P. Reyes, R. H. Heffner, P. C. Canfield, S-W. Cheong, Z. Fisk, and J. E. Schirber, Physica C **185-189**, 1095 (1991).
[16] M. F. Hundley, J. D. Thompson, S-W. Cheong, Z. Fisk, and J. E. Schirber, Phys. Rev. B **41**, 4062 (1990).
[17] L. L. Miller, K. Sun, D. C. Johnston, J. E. Schirber, and Z. Fisk, J. Alloys Compounds **183**, 312 (1992).
[18] V. J. Emery, S. A. Kivelson, and H. Q. Lin, Phys. Rev. Lett. **64**, 475 (1990); S. A. Kivelson, V. J. Emery, and H. Q. Lin, Phys. Rev. B **42**, 6523 (1990).
[19] V. J. Emery and S. A. Kivelson, Physica C **209**, 597 (1993).
[20] T. Thio, T. R. Thurston, N. W. Preyer, P. J. Picone, M. A. Kastner, H. P. Jenssen, D. R. Gabbe, C. Y. Chen, and R. J. Birgeneau, Phys. Rev. B **38**, 905 (1988).
[21] S. W. Lovesey, *Theory of Neutron Scattering from Condensed Matter* (Oxford Science Publications, Oxford, 1987), Vol. 1.
[22] A. Junod, in *Physical Properties of High Temperature Superconductors II*, edited by D. M. Ginsberg (World Scientific, Singapore, 1990), Chap. 2, pp. 13–120.
[23] P. G. Radaelli, J. D. Jorgensen, B. Kleb, B. W. Hunter, F. C. Chou, and D. C. Johnston (unpublished).
[24] D. Vaknin, E. Caignol, P. K. Davies, J. E. Fischer, D. C. Johnston, and D. P. Goshorn, Phys. Rev. B **39**, 9122 (1989).
[25] D. Vaknin, S. K. Sinha, C. Stassis, D. C. Johnston, and L. L. Miller, Phys. Rev. B **41**, 1926 (1990).
[26] We determine this upper limit to the resolution from the the (200) reflection that has the nominal position (100) due to the $\lambda/2$ contamination of the neutron beam.
[27] J. Ryder, P. A. Midgley, R. Exley, R. J. Beynon, D. L. Yates, L. Afalfiz, and J. A. Wilson, Physica C **173**, 9 (1991).